Supporting Information

Chen et al. 10.1073/pnas.1001745107

SI Materials and Methods

Generation of Purkinje Neuron–Specific BK$^{-/-}$ Mice. For establishing a mouse line with a tissue-specific deletion of BK channel α-subunit in Purkinje neurons (PN-BK$^{-/-}$), constitutive heterozygous BK L1/+ mice (SV129 background) were intercrossed with transgenic mice expressing the Cre recombinase under the control of the Purkinje protein 2 (PNP2) gene, which is thought to be specifically expressed in PNs and in retinal bipolar neurons (1). The generation of this PNP2-Cre mouse line was described in detail by Barski et al. (1). Progenies both carrying one BK L1 allele and being transgenic for PNP2-Cre were then crossed with mice carrying two *loxP*-flanked L2 alleles (BK L2/L2; SV129 background) of the BK gene *KCNMA1* (2) to obtain PNP2-Cre transgenic BK L2/L1 (PN-BK$^{-/-}$) and PNP2-Cre transgenic BK L2/+ (PN-BK-Control) mice. The correct genotype was analyzed by PCR amplification as described previously (Fig. S1) (1, 2).

Mice were bred and maintained at the animal facility of the Institute of Pharmacy, Department Pharmacology and Toxicology, University of Tübingen, Germany. Either litter- or age-matched mice (at an age of 3 to 4 months) were randomly assigned to the experimental procedures with respect to the German legislation on animal protection. All experimental procedures were performed in accordance with institutional animal welfare guidelines and were approved by the state government of Bavaria, Germany.

Immunohistochemistry and Silver Staining. Mice were killed in a CO_2 chamber and perfused with 50 mM PBS (ice-cold), followed by 4% PFA in PBS (ice-cold) for 4 min. Brains were removed, incubated in ascending concentrations of sucrose (5% 1 h/10% 12 h/20% 24 h) and snap frozen at −80 °C in isopentane. Immunohistochemistry was conducted as described previously (3). Briefly, free-floating coronal cryostat sections (40 μm) were permeabilized in three changes (20 min each) of Tris-buffered saline (TBS; 100 mM Tris/HCl and 150 mM NaCl, pH = 7.4) with 0.2% Triton X-100 (TBS-T). Endogenous peroxidases were blocked in 25% methanol and 0.6% H_2O_2 in TBS for 20 min. Samples were washed once in TBS and twice in TBS-T. Protein blocking was conducted with 2% BSA and 2% normal goat serum in TBS-T for 1 h. Samples were incubated with mouse monoclonal anti-BKα$_{(690\text{-}715)}$ antibody (1:1,000; NeuroMab Clone L6/60) in TBS-T/1% BSA overnight at 4 °C, washed thrice with TBS-T (20 min each), and incubated with HRP-tagged goat anti-mouse antibody (1:300; DAKO P0447) for 2 h. After three washes with TBS, slices were developed using the standard diaminobenzidine method. Sections were mounted on gelatin-coated slices in 60% ethanol, dried on a hot plate (60 °C) for 15 min, dehydrated in 96% and 100% ethanol, cleared in xylene, and sealed in Entellan. Imaging was performed using a Zeiss Axioplan II microscope equipped with an AxioCam digital color camera (Fig. S1).

Silver staining was performed using a modified Sevier-Munger procedure. Free-floating cryostat sections were postfixed in 4% formalin in water (15 min) and washed thrice in deionized water. Sections were incubated in 20% silver nitrate for 15 min at 60 °C, rinsed once in deionized water, and developed in ammoniacal silver solution (10%) containing sodium bicarbonate and formalin. Samples were rinsed in distilled water, and excess silver was removed in 5% sodium thiosulfate for 10 min. Mounting, dehydration, and sealing were conducted as described above.

Behavioral Tests. ***Footprint pattern.*** Paw positions were recorded while mice were walking on a glass plate with a video camera position underneath the plate (4).

Ladder walking test. The horizontal ladder walking test was similar to the one designed for testing rats described previously (5). The ladder runway was composed of 38 rods with a diameter of 2 mm positioned at intervals of 2 cm. Each test consisted of at least two runs on the ladder. Slips of the fore- and hindlimbs were counted.

Elevated bar balancing test. The setup consisted of a 50 × 1-cm bar that connected two platforms located 50 cm above the ground. The animals were placed perpendicularly onto the bar and had to move toward one end until they reached a platform. This procedure was repeated to observe at least 20 walking steps. Both fore- and hindlimb slips from the bar were counted.

The trials were filmed at a rate of 30 frames per second using a digital video camera and analyzed frame by frame off-line. Statistical analysis was performed by using the Mann-Whitney *U* test (ladder walking, elevated bar) or χ^2 test (footprint pattern).

In Vivo Electrophysiological Recordings. Adult mice (1–4 months old) were used in all of the experiments. Surgery was performed in accordance with institutional animal welfare guidelines as described previously (6, 7). Briefly, the mice were placed onto a warming plate (38 °C) and anesthetized by inhalation of 1.5% isoflurane (Curamed) in pure O_2. The depth of anesthesia was assessed by monitoring the tail-pinch reflex and the respiration rate. After locally applying an anesthetic agent (xylocaine), the skin and muscles were removed under a dissecting microscope. A custom-made recording chamber was then glued to the skull with cyanoacrylic glue (UHU). A rectangular craniotomy (2.5 mm × 4.0 mm) was made using a high-speed drill with a small-tip steel burr (0.5 mm in diameter) to expose the cerebellar vermis (coordinates: Bregma −5.5 to −7.5 mm, ±1 mm lateral to the midline) (8). The craniotomy was then filled with 1.5% low-melting-point agarose (Sigma) to minimize brain pulsations. After surgery, the mouse was transferred into the recording setup and continuously supplied, through a face mask, with 0.8–1.2% isoflurane in pure O_2. The recording chamber was perfused with warm (36.5 °C) normal Ringer's solution containing (in millimolars) 125 NaCl, 4.5 KCl, 26 $NaHCO_3$, 1.25 NaH_2PO_4, 2 $CaCl_2$, 1 $MgCl_2$, and 20 glucose, pH 7.4, when bubbled with 95% O_2 and 5% CO_2. During surgical and recording procedures, the rectal temperature of mouse was maintained at 36.5–37.5 °C with a warming plate.

Somatic cell-attached patch-clamp recordings were obtained with an EPC9/2 amplifier (HEKA Elektronik) under two-photon imaging. Two-photon imaging was performed with a custom-built video-rate two-photon microscope based on a resonance scanner (9) and a mode-locked femto-second pulse laser, operating at 710–920 nm wavelength (MaiTai; Spectra Physics). The scanner was mounted on an upright microscope (BX61WI; Olympus) equipped with a ×40/0.80-W water-immersion objective (Nikon). A patch pipette filled with normal Ringer's solution containing 50 μM Alexa594 (Invitrogen) had a tip resistance of 4–6 MΩ. The details of the shadow-patching process for PNs were described previously (10). After recording, some cells were fluorescently labeled by using targeted single-cell electroporation (10). The identity of PNs was confirmed by the reconstructed projection images of dye-filled cells. 3D reconstructions were performed using either ImageJ (http://rsbweb.nih.gov/ij/) or Amira (http://www.amiravis.com/). In some experiments, cell-attached recordings to monitor climbing fiber activity using both electrical and dendritic Ca^{2+} measurements were performed in PNs that were prelabeled with Oregon Green BAPTA-1 via electroporation (10). For local drug application to PNs, a glass pipette filled with Alexa594 and the corresponding drug was

placed near (20–50 μm) the dendrites of a PN under two-photon imaging guidance. The drug and Alexa594 were coreleased by gentle pressure application (Picospritzer III; General Valve).

Electrophysiological data were filtered at 10 kHz and sampled at 20–50 kHz using Pulse software (HEKA). Simple and complex spikes (SS and CS) from extracellular recordings were sorted according to their amplitudes, shapes, and time courses using Igor Pro (Wavemetrics) in conjunction with the Neuromatic software package (version 2.00) and a custom-written macro. A 1-s or a 10-s time window was used for detecting events and for computing the frequency of SS or CS, respectively. Statistical analysis was performed with SPSS 10.0 for Windows (SPSS).

1. Barski JJ, Dethleffsen K, Meyer M (2000) Cre recombinase expression in cerebellar Purkinje cells. *Genesis* 28:93–98.
2. Sausbier M, et al. (2004) Cerebellar ataxia and Purkinje cell dysfunction caused by Ca^{2+}-activated K^+ channel deficiency. *Proc Natl Acad Sci USA* 101: 9474–9478.
3. Sausbier U, et al. (2006) Ca^{2+} -activated K^+ channels of the BK-type in the mouse brain. *Histochem Cell Biol* 125:725–741.
4. Hartmann J, et al. (2008) TRPC3 channels are required for synaptic transmission and motor coordination. *Neuron* 59:392–398.
5. Metz GA, Whishaw IQ (2002) Cortical and subcortical lesions impair skilled walking in the ladder rung walking test: A new task to evaluate fore- and hindlimb stepping, placing, and co-ordination. *J Neurosci Methods* 115:169–179.
6. Rochefort NL, et al. (2009) Sparsification of neuronal activity in the visual cortex at eye-opening. *Proc Natl Acad Sci USA* 106:15049–15054.
7. Stosiek C, Garaschuk O, Holthoff K, Konnerth A (2003) In vivo two-photon calcium imaging of neuronal networks. *Proc Natl Acad Sci USA* 100:7319–7324.
8. Franklin K, Paxinos G (2001) *The Mouse Brain in Stereotaxic Coordinates* (Academic Press Inc., San Diego).
9. Leybaert L, de Meyer A, Mabilde C, Sanderson MJ (2005) A simple and practical method to acquire geometrically correct images with resonant scanning-based line scanning in a custom-built video-rate laser scanning microscope. *J Microsc* 219:133–140.
10. Kitamura K, Judkewitz B, Kano M, Denk W, Häusser M (2008) Targeted patch-clamp recordings and single-cell electroporation of unlabeled neurons in vivo. *Nat Methods* 5:61–67.

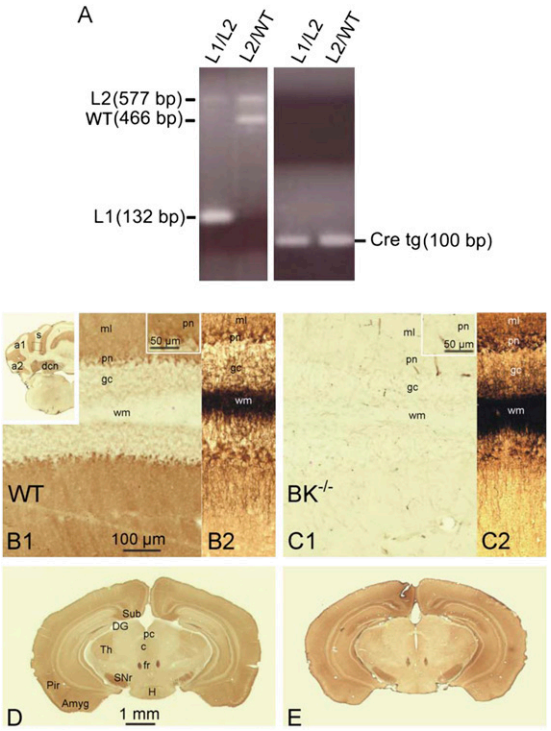

Fig. S1. Genotyping of Purkinje neuron–specific $BK^{-/-}$ mice (PN-$BK^{-/-}$) and immunohistochemistry. (*A*) PCR was used to genotype PN-$BK^{-/-}$ (PCP2-Cre tg BK L1/L2) and control (PCP2-Cre tg BK L2/WT) mice. (*B1, C1*) Immunostaining for BK channels in the cerebellar cortex of WT (*B1*) and PN-$BK^{-/-}$ (*C1*) mice. In WT, strong staining was observed in the PN layer (pn) containing the cell bodies of PNs and the molecular layer (ml) containing their dendrites. In line with previous reports (1, 2), the staining in the granule cell layer (gc) was weak. In PN-$BK^{-/-}$, staining in the pn and ml was strongly reduced. *Left Inset:* rectangle depicts region shown in *B* and *C*. a1/a2, ansiform lobule crus1/2; S, simple lobule; dcn, deep cerebellar nuclei; wm, white matter. *Right Insets:* PNs are readily seen in WT mice (*B1*) but not in PN-$BK^{-/-}$ mice (*C1*). (*B2*, *C2*) Silver staining shows that PNs can be observed in both WT (*B2*) and PN-$BK^{-/-}$ mice (*C2*). (*D* and *E*) Immunostaining for BK channels in the whole brain. In both WT (*D*) and PN-$BK^{-/-}$ (*E*) mice, strong BK channel expression was seen in different regions. Amyg, amygdala; Pir, piriform cortex; Th, thalamus; DG, dentate gyrus; Sub, subiculum; SNr, substantia nigra, pars compacta; H, hypothalamus; c: central gray matter (periaqueductal gray); fr, fasciculus retroflexus; pc, posterior commissure.

1. Barski JJ, Dethleffsen K, Meyer M (2000) Cre recombinase expression in cerebellar Purkinje cells. *Genesis* 28:93–98.
2. Sausbier M, et al. (2004) Cerebellar ataxia and Purkinje cell dysfunction caused by Ca^{2+}-activated K^+ channel deficiency. *Proc Natl Acad Sci USA* 101:9474–9478.

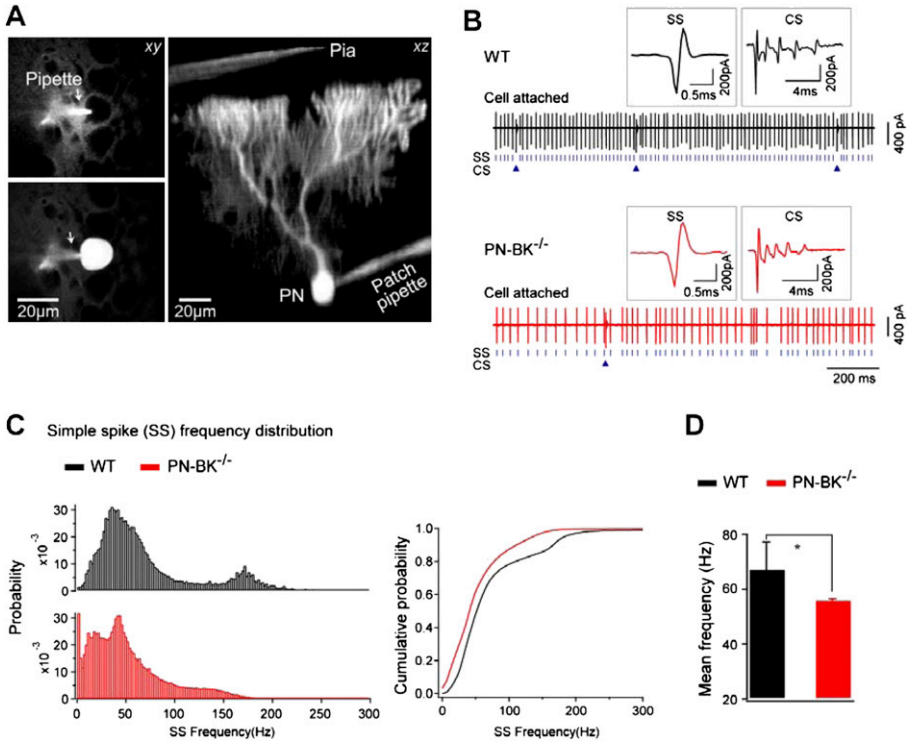

Fig. S2. Reduction in simple spike firing in PNs of PN-BK$^{-/-}$. (*A*) Visual identification of PN using in vivo two-photon imaging. A pipette filled with Alexa594 (50 μM) (arrow) was attached to the soma of a PN before (*Upper Left*) and after (*Lower Left*) electroporation. *Right: xz* projection showing the reconstruction of an electroporated PN. (*B*) Representative cell-attached recording from a WT (*Upper*, black) or PN-BK$^{-/-}$ (*Lower*, red) PN. *Insets:* SS and CS waveforms from both genotypes. (*C*) *Left:* Distribution of SS instantaneous frequency in WT (black) and PN-BK$^{-/-}$ (red) mice (bin = 2 Hz). *Right:* Cumulative distribution calculated from *Left* showing left-shift of SS frequency in PN-BK$^{-/-}$. (*D*) Comparison of mean frequency of SS in WT (black) and PN-BK$^{-/-}$ (red). The mean frequency was calculated from 2-min recording for each cell. (n = 34 WT cells and 57 PN-BK$^{-/-}$ cells in 10 mice for each genotype.) *P < 0.05. Error bars show SEM.

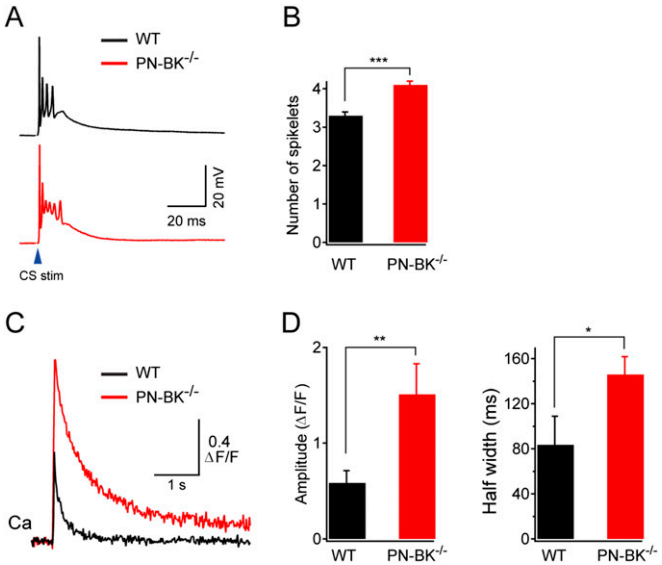

Fig. S3. Changes of complex spike waveform and complex spike-associated dendritic Ca^{2+} transient in PNs of PN-BK$^{-/-}$ in slice preparation. (*A*) Representative complex spikes from WT (*Upper*, black) and PN-BK$^{-/-}$ (*Lower*, red) mice. (*B*) Comparison of spikelets number of CS between WT (black) and PN-BK$^{-/-}$ (red) (30 CSs; 6 CSs from each cell; n = 5 cells for each genotype.) ***P < 0.001. Error bars show SEM. (*C*) Averaged climbing fiber–evoked Ca^{2+} transients from WT (black) and PN-BK$^{-/-}$ (red). Each trace was averaged from five events (each event from each cell; n = 5 cells for each genotype). (*D*) Comparison of the amplitude (*Left*) and half width (*Right*) of Ca^{2+} transient in WT (black) and PN-BK$^{-/-}$ (red) (20 Ca^{2+} transients, 4 Ca^{2+} transients from each cell; n = 5 cells for each genotype). **P < 0.01; *P < 0.05. Error bars show SEM.

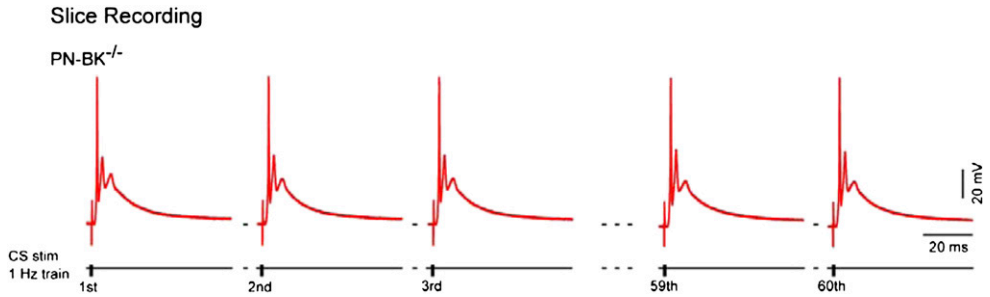

Fig. S4. Stable complex spike waveform during repetitive stimulation in PNs of PN-BK$^{-/-}$ mice. Current-clamp recordings were performed in cerebellar slice preparations. Complex spikes were elicited by a stimulation electrode placed in the granule layer. Sixty consecutive complex spikes were recorded in response to 1 Hz stimulation. Note that no detectable difference was found between the first and the 60th CS. Similar results were obtained in six PNs.

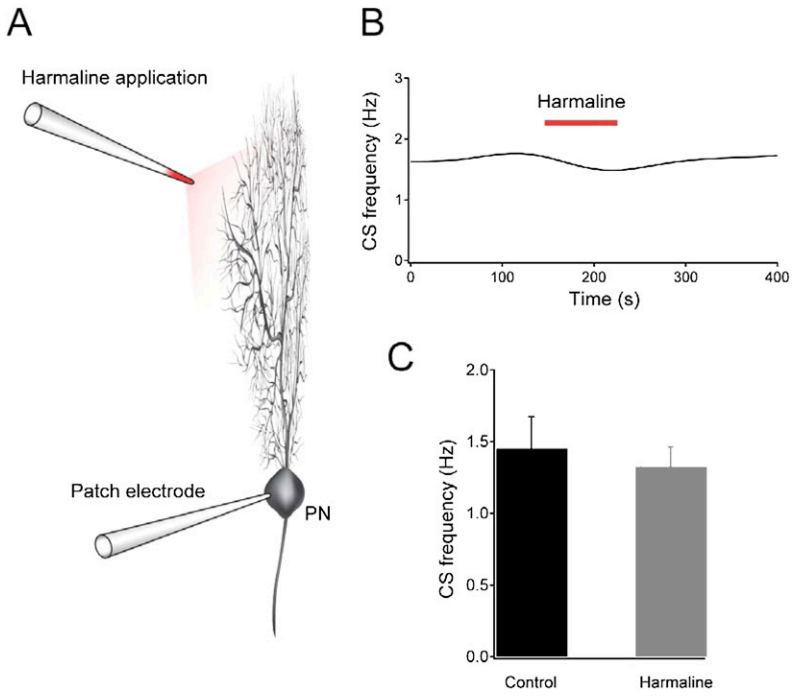

Fig. S5. No significant effect of harmaline on CS frequency by local application to the recorded PN in vivo. (*A*) Schematic presentation showing the experimental design. The glass pipette for drug application was filled with both Alexa594 and harmaline. The patch electrode is shown for cell-attached recording. Before performing cell-attached recording and placing the drug pipette, the cell was labeled with Alexa594 by electroporation. (*B*) Example of the time course showing no effect of harmaline on CS frequency in one cell. (*C*) Summary of data in *B*, showing the average CS frequency before and during harmaline application (n = 4 PNs). Error bars show SEM.

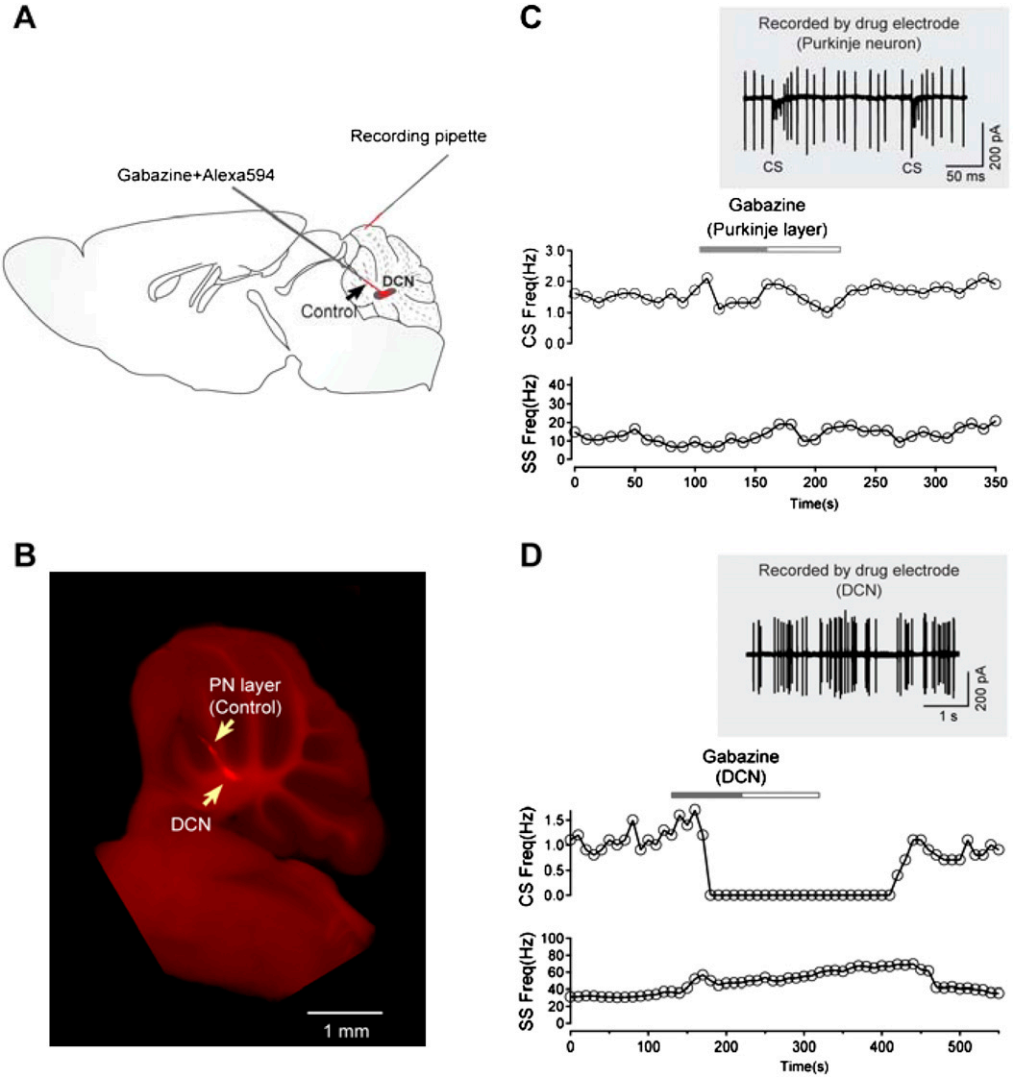

Fig. S6. Control for the site-specific action of gabazine application to the deep cerebellar nuclei (DCN). (*A*) Experimental configuration for cell-attached recordings from PNs and local drug application (gabazine, 200 μM) to the DCN and to a control location (arrow) near the DCN. (*B*) Fluorescence image of an acute slice preparation with the tract of the gabazine and Alexa594-containing pipette. The slice was obtained immediately after the end of the in vivo recordings (see *SI Materials and Methods*). The arrows indicate the approximate sites of gabazine application: first, the cerebellar PN layer, approximately 500 μm away from the DCN (*C*) and, second, the DCN (*D*). Note that the position of the recording patch-pipette (not shown) was in a different plane of focus, approximately 2.5 mm away from the DCN. (*C*) Local application of gabazine at the site of PN layer (marked in *B*) had no detectable effect on CS and SS activities recorded by the recording pipette (location indicated in *A*). Before gabazine injection, the location of PN layer was identified by the drug pipette-based recording of the characteristic CS activity from one PN (*Inset*). (*D*) Local application of gabazine to the DCN blocked the CS and increased the SS activity. Before gabazine application, the spontaneous activity of a DCN neuron was monitored by the drug pipette in the loose cell-attached configuration (*Inset*). These results verify the specificity of the gabazine application to the DCN.

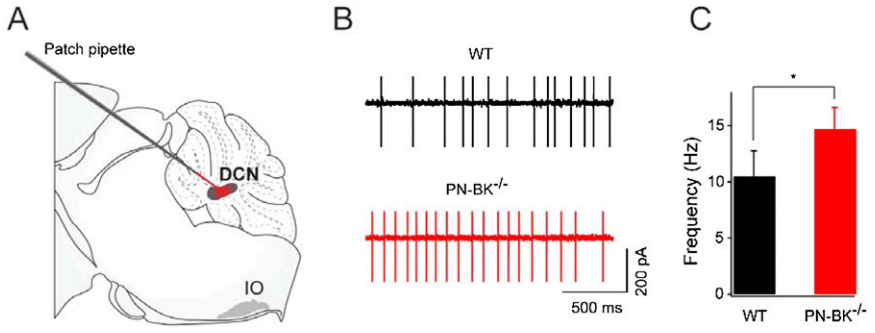

Fig. S7. Increased activity in deep cerebellar nuclei (DCN) neurons PN-BK$^{-/-}$ mice in vivo. (*A*) Experimental configuration for extracellular recordings in DCN neurons in vivo. (*B*) Examples of extracellular activity from DCN neurons in WT (*Upper*, black) and PN-BK$^{-/-}$ (*Lower*, red). The spikes are truncated in amplitude. (*C*) Comparison of mean frequency of DCN neuron activity in both genotypes (n = 16 WT cells and 14 PN-BK$^{-/-}$ cells). *$P < 0.05$. Error bars show SEM.

Table S1. Summary of mean frequencies of CS and SS in WT and PN-BK$^{-/-}$ and effects of various pharmacological interventions

Treatment	Spike type	Subtype	Mean frequency (Hz)			
				PN-BK$^{-/-}$		WT
None	SS	—		55.6 ± 1.0* (n = 57)		67.0 ± 10.3 (n = 34)
	CS	Normal		1.07 ± 0.08* (n = 18)		1.45 ± 0.06 (n = 32)
		Quiet		0.15 ± 0.03 (n = 13)		0.45 ± 0.08 (n = 2)
		Silent		0 (n = 26)		Not detected
Gabazine	CS	Not determined		Not tested	Before	1.60 ± 0.14 (n = 8)
					During	0.43 ± 0.16‡ (n = 8)
Muscimol	CS	Normal	Before	1.36 ± 0.08 (n = 5)	Before	1.55 ± 0.12 (n = 11)
			During	1.52 ± 0.09* (n = 5)		
		Quiet	Before	0.27 ± 0.09 (n = 7)		
			During	0.50 ± 0.12† (n = 7)	During	1.63 ± 0.15 (n = 11)
		Silent	Before	0 (n = 7)		
			During	0.11 ± 0.01‡ (n = 7)		
Harmaline	CS	Not determined	Before	0.41 ± 0.08 (n = 18)	Before	1.26 ± 0.13 (n = 7)
			During	4.07 ± 0.31‡ (n = 10)	During	3.98 ± 0.21† (n = 13)

*$P < 0.05$; †$P < 0.01$; ‡$P < 0.001$ vs. WT or before drug application.